Acta Oceanol. Sin., 2025, Vol. 44, No. 2, P. 24–36
https://doi.org/10.1007/s13131-024-2371-2

Remote sensing monitoring for impact of island on chlorophyll *a* in the water near the Diaoyu Island (Diaoyu Dao) and its affiliated islands, China

Lina Cai[1], Ruohao Xin[1], Xiaomin Ye[2*], Rong Tang[1], Jie Yin[1], Leichao Cheng[1]

[1] Marine Science and Technology College, Zhejiang Ocean University, Zhoushan 316022, China
[2] National Satellite Ocean Application Service, Beijing 100081, China

Received 6 May 2024; accepted 4 July 2024

Abstract

The Diaoyu Island (Diaoyu Dao) and its affiliated islands (DAA) have abundant fishery resources, and chlorophyll *a* (Chl *a*) concentration is an important marine color element and an important indicator of primary productivity in the ocean. Therefore, it is meaningful to understand the distribution and variation characteristics of Chl *a* concentration in the waters near the DAA. The distribution details of Chl *a* concentration in the adjacent waters of DAA were revealed by high-resolution satellite GF-1 Wide Field View (WFV) data with 16 m spatial resolution. The results indicate that: (1) The Chl *a* concentration is between 0.06 μg/L and 0.38 μg/L throughout the year and the concentration of Chl *a* in the northeast and east directions of the island (downstream) is significantly higher than that in the west (upstream), and there are observed vortexes with high Chl *a* concentration in the downstream of DAA. This phenomenon continues to persist in the waters surrounding the DAA all year. (2) The vortex induced by the interaction between the current and island results in the vorticity change of water, inducing the replenishment of a large number of nutrients to the surface, thereby promoting the growth of plankton in the downstream of DAA on the east. In addition, the DAA also plays a significant role in regulating the downstream mix layer depth (MLD). The MLD in the northeast downstream is considerably deeper than the upstream in winter and spring; it is deeper in the east downstream in summer and autumn, and the range of influence for the MLD is greatly larger than the size of the island itself. This shows that the disruption of the DAA on the current is substantial. In addition, the combined effects of SST and wind also play a significant role in modifying Chl *a* distribution. (3) Based on the analysis above, this study proposes the conception of building fishing pastures downstream of the DAA, and proposes a general migration plan in different seasons to scientifically and rationally utilize and protect the surrounding waters of DAA.

Key words Diaoyu Island and its affiliated islands, high-resolution satellite, chlorophyll *a*

Citation Cai Lina, Xin Ruohao, Ye Xiaomin, Tang Rong, Yin Jie, Cheng Leichao. 2025. Remote sensing monitoring for impact of island on chlorophyll *a* in the water near the Diaoyu Island (Diaoyu Dao) and its affiliated islands, China. Acta Oceanologica Sinica, 44(2): 24–36, doi: 10.1007/s13131-024-2371-2

1 Introduction

Islands play a crucial role in the global sea system, as interact with surrounding waters causing changes in the ecology and hydrological environment of the surrounding seas (Gove et al., 2016). Research on the effects of the island on the surrounding waters can be conducive to improving the management of associated marine engineering and industries, such as fishery, marine aquaculture, coastal engineering, and others (Xu et al., 2019; Nielsen et al., 2019). Early research discovered that islands can induce the island mass effect (IME) in numerous locations around the world, which could cause localized increases of phytoplankton due to the presence of the island (Doty and Oguri, 1956). Observations have been made around islands of different sizes in various regions around the world (Lamont and Toolsee, 2022; Vollbrecht et al., 2021; Chiswell and O'Callaghan, 2021). This is a common phenomenon

Foundation item: The Basic Public Welfare Research Program of Zhejiang Province under contract No. LGF21D010004; the Key R&D Projects in Zhejiang Province under contract No. 2023C03120.
*Corresponding author, E-mail: yxm@mail.nsoas.org.cn

in marine island systems. The primary productivity of the sea area where IME occurs will be improved to a certain extent, which is conducive to the scientific selection and management of fishing grounds. Therefore, the scientific community consistently devoted attention to the mechanism of IME brought about by islands. Many studies have suggested that this process is controlled by dynamic and biological coupling (Gao et al., 2022; Hasegawa et al., 2009). The interaction between islands and surrounding oceans or atmospheric systems will induce vortices, change sea surface temperature (SST), affect water stability, and change wind shear stress (Yoshida et al., 2010), which will affect the growth and reproduction of plankton and, consequently, affect the concentration of chlorophyll *a* (Chl *a*) (Hasegawa et al., 2008; Liu and Chang, 2018).

As the satellite technology and the retrieved model continue to mature, numerous scholars employ satellite data to monitor Chl *a*, and other seawater color data, such as suspended sediment distribution (Cai et al., 2020, 2022), SST (Hsu et al., 2017), and sea surface texture (Cai et al., 2023). Nevertheless, high-resolution studies are scarce regarding the seawater color of the Diaoyu Island (Diaoyu Dao) and its affiliated islands (DAA).

The DAA is located in the northeast of Taiwan Island, China, spanning the sea at 25°40′–26°00′N and 123°20′–124°40′E, which comprises Diaoyu Island, Huangwei Islet (Huangwei Yu), Chiwei Islet (Chiwei Yu), Nanxiao Island (Nanxian Dao), Beixiao Island and many uninhabited islands such as Nan Islet (Nan Yu), Bei Islet (Bei Yu), and Fei Islet (Fei Yu), covering an estimated land area of 5.69 km^2 (Fig. 1). The island is situated in the Kuroshio basin. According to previous studies, islands will interact with the surrounding environment and induce obvious changes in the biochemical and physical properties of the surrounding ocean. However, there is limited research and explanation regarding the interaction between the DAA and its surrounding environment. Moreover, DAA is abundant in fishery resources (Ma et al., 2012). The Chl *a* concentration is the significant proxy of the concentration of the primary productivity and phytoplankton, which constitute the base of the marine food net (Roxy et al., 2016), so the Chl *a*'s distribution and seasonal changes of the concentration are closely related to the development of fishery resources in the vicinity of the island; however, they remain to be elucidated.

The main novelty of this study lies in the application of GF-1 Wide Field View (WFV) data with 16 m spatial resolution to retrieve the distribution and change details of Chl *a* concentration around the DAA, and to reveal the impact of the islands on Chl *a* distribution. The study contributes to a better understanding of the marine environment around the DAA and provides a scientific basis for its effective management.

2 Data and methods

2.1 *Study area*

DAA includes uninhabited islands such as Huangwei Islet, Chiwei Islet, Nanxiao Island, Beixiao Island, Nan Islet, Bei Islet and many reefs (Fig.1c). It is approximately 150 km from the Ryukyu Islands to the south, separated by the deep Okinawa Trough. The DAA includes uninhabited islands such as DAA, Huangwei Islet, Chiwei Islet, Nanxiao Island, Beixiao Island, Nan Islet, Bei Islet and many reefs (Fig. 1c). The total area is about 5.69 km^2, of which the DAA is the largest, about 3.9 km^2. There is a wide shallow sea area near the shore of the DAA, where a wide underwater shoal is developed and connected with the shoal around the island. The olive gate between the Beixiao Island and the Nanxiao Island is about 10 m deep and 200 m wide. The near-shore shallow sea area (30 m shallow) of the two islands is connected into one, the southwest side is narrow, and the northeast side extends nearly 2 km, during which a series of tidal creeks are distributed (Fig. 1b). There are a large number of tidal creeks and reef flats perpendicular to the coast on the southwest and northeast sides of the Bei Islet (China).

2.2 *Data*

The study mainly uses high-resolution remote-sensing data of the near sea of DAA from the WFV sensor of GF-Diaoyu Island (Diaoyu Dao) and its affiliated islands (DAA) (Table 1). The GF-1 satellite was launched on 26 April 2013. GF-1 with a sun-synchronous orbit with an altitude of 645 km expect service life of five to seven years, and it crosses the equator at 10:30 local time with a descending mode (Xu et al., 2020; Mattei and Scardi, 2022).

Hydrological data, involving SST, current, wind, MODIS Chl *a* concentration, and mixes layer depth (MLD), were applied to analyze and discuss the distribution and variation of Chl *a* around DAA (Rosa et al., 2022). Seasonal climatology and annual SST data were retrieved from MODIS data (https://oceancolor.gsfc.nasa.gov/). Wind data were from fifth generation ECMWF reanalysis data (https://www.ecmwf.int/). Current data were from Global Ocean Forecasting System (https://www.hycom.org/). Monthly Chl *a* data retrieved from MODIS data were used to analyze the general distribution of Chl *a* in the DAA sea (https://oceancolor.gsfc.nasa.gov/). MLD data were from the Operational Mercator Global Ocean Analysis and Forecast System (https://data.marine.copernicus.eu/). The resolution information of the relevant data was organized in Table 2.

2.3 *Data processing*

The preprocessing of remote sensing data includes radiometric calibration, atmospheric correction, and orthorectified correction. In this research, the approach of preprocessing the GF-1 WFV data was achieved in software ENVI 5.3, which was chosen by many scholars to process the kinds of satellite data (Qin et al., 2014; Song et al., 2012). The first step is multispectral data processing. The radiometric calibration used the radiometric calibration module to transfer the DN number value to

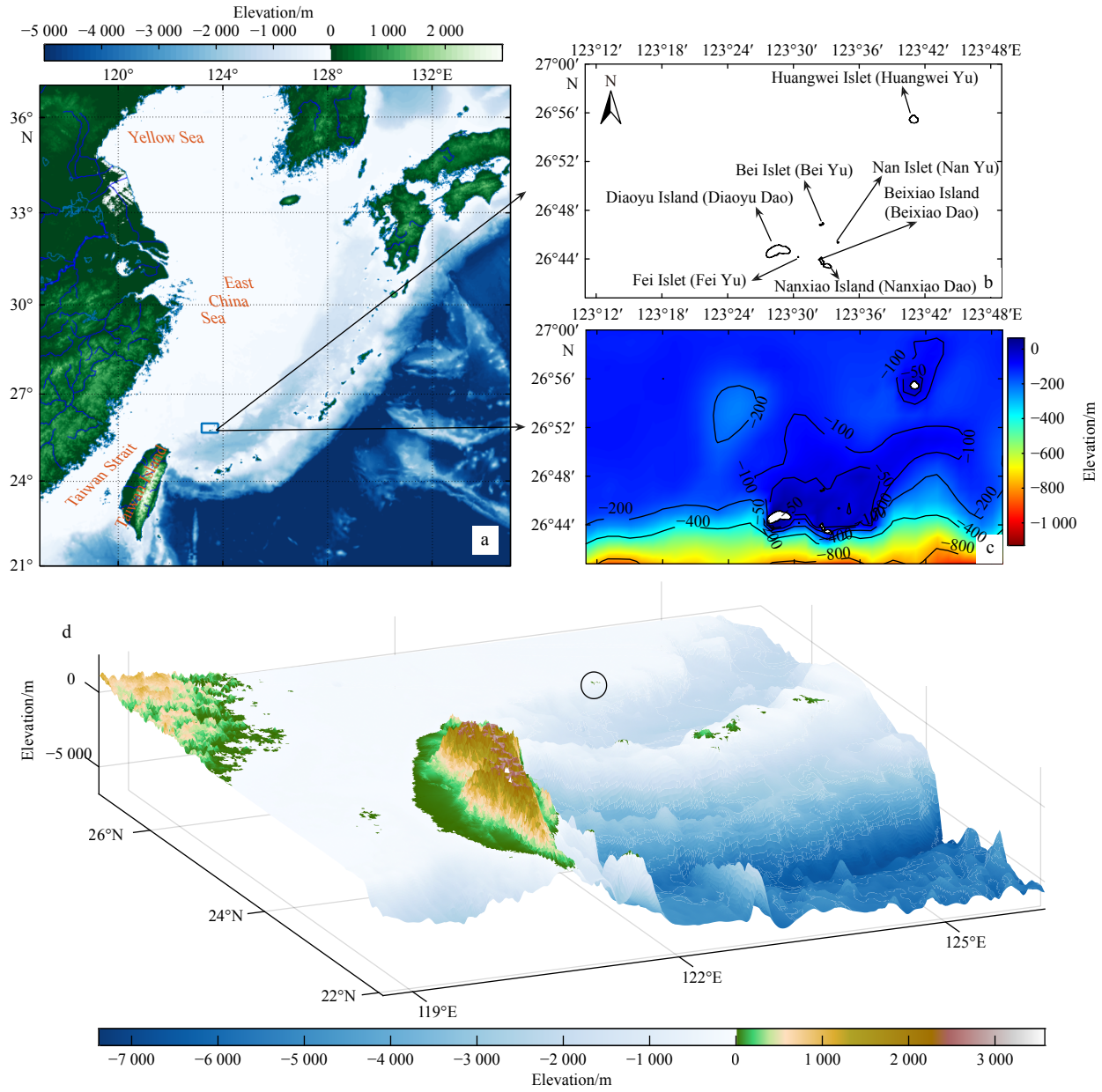

Fig. 1. Location around the waters of the Diaoyu Island. a, b and c. The elevation of the surrounding larger-scale areas (a) and smaller-scale areas (b and c). The region circled by blue rectangle in a implies the b and c area. d. Topographic map of the area around DAA from a three-dimensional perspective, and the DAA circled by elliptical.

Table 1. The parameters of GF-1 WFV data

Sensor	Band	Wavelength/μm	Resolution/m
GF-1 WFV	Band1 (blue)	0.45–0.52	16
	Band2 (green)	0.52–0.59	16
	Band3 (red)	0.63–0.69	16
	Band4 (near infrared)	0.77–0.89	16

Table 2. The source of the hydrological data

Name	Resolution
Seasonal climatology SST	4 km × 4 km
Annual SST	4 km × 4 km
Wind	0.25° × 0.25°
Current	0.08° × 0.08°
MODIS Chl *a*	4 km × 4 km
MLD	0.08° × 0.08°

reflectance. The conduction of atmospheric correction is aimed at reducing the influence of the reflection and scattering caused by Aerosol and Rayleigh scattering (Cai et al., 2020) by the fast line-of-sight atmospheric analysis of spectral hypercubes (FLAASH) model (Felde et al., 2003). The former study demonstrated that the FLAASH was performed to estimate surface reflectance for atmospheric absorption and scattering effect, based on the moderate spectral resolution atmospheric transmittance (MODTRAN) radiative transfer approach (Anderson et al., 1999). In this step, the tropic model was chosen for the atmospheric model. The aerosol model chose the maritime. The former study demonstrated that or-

thorectified correction can correct spatial accuracy (Peng et al., 2019).

2.4 *High-resolution Chl a retrieval model*

High-resolution spatial-temporal observation was conducted in the offshore waters of DAA to analyze the distribution and variation of Chl *a*. The DAA is located in the ECS, near the northern South China Sea (NSCS). According to Shang et al. (2014), the OC3M (ocean chlorophyll three-band algorithm for MODIS) model has a good inversion effect in this NSCS with a coefficient of determination (R^2) of 0.81 and a root mean square error (RMSE) on the log scale of 0.363 (Shang et al., 2014). Many studies of tropical sea areas at similar latitudes have chosen this model when retrieving the Chl *a* data (Andrade et al., 2014b; Zheng and Li, 2022). The study also selects the OC3M as the inversion model and the equation is as follow:

$$C = 10^{0.242-2.743x+1.801\,7x^2+0.001\,5x^3-1.228x^4}, \tag{1}$$

$$x = \log_{10}\left(\frac{\mathrm{Max}\left(R_{\mathrm{rs}}(443), R_{\mathrm{rs}}(488)\right)}{R_{\mathrm{rs}}(547)}\right), \tag{2}$$

and the x for GF-1 WFV data is:

$$x = \log_{10}\left(\frac{R_{\mathrm{rs}}(450)}{R_{\mathrm{rs}}(520)}\right), \tag{3}$$

where C is the Chl *a* concentration in μg/L, $R_{\mathrm{rs}}(450)$ and $R_{\mathrm{rs}}(520)$ are the reflectance of the WFV data in blue and green bands, respectively.

3 Results

3.1 *The general Chl a distribution pattern in the waters around DAA*

By utilizing the MODIS seasonal climatology Chl *a* concentration data obtained from 2002 to 2023 (Fig. 2), we can conclude that the Chl *a* concentration around the DAA is highest in winter and lowest in summer, with generally in the range of 0.06−0.38 μg/L. The Chl *a* average level is generally in the range of 0.18−0.38 μg/L during winter (Fig. 2, winter), 0.1−0.3 μg/L during spring (Fig. 2, spring), 0.06−0.22 μg/L during summer and autumn (Fig. 2, summer, autumn). The distribution of high values is generally in the north and east, while the low values typically are found in the south and west. And the high Chl *a* concentration abnormal value often appears in winter (Fig. 2, winter; and Fig. 3, winter).

3.2 *Details of the Chl a concentration change in the adjacent area of the DAA*

High-resolution Chl *a* concentration retrieved from GF-1 WFV data, as illustrated in Fig. 4, revealed Chl *a* distribution details. Chl *a* concentration in the downstream of the island in the east is significantly higher than that in the upstream in the west. The vortexes downstream of DAA with a high concentration of Chl *a* in various development stages, including the newly born vortex with a size similar to the island (Fig. 4f) and the mature Karman vortex street (Fig. 4e) are captured. The Chl *a* concentration in the center of the vortex is high, and the high concentration of Chl *a* decreases gradually with the length of Karman vortex street (Fig. 4). The distribution direction of high-value areas downstream of the island varies during different seasons, but the dominant direction is east. In the summer and autumn, the high-value areas are mainly located in the northeastern region downstream of the island (Figs 4a, b, c, d, and e), and in the winter, they are mainly located on the eastern side of the downstream of the island (Fig. 4f). Combined with Fig. 2, in large-scale spatial scales, the increment of Chl *a* concentration in the downstream of the DAA, can also be discovered in different season (Fig. 3: 2014 spring, 2018 summer, 2017 autumn, and 2018 winter). In addition, areas of low values have been discovered in the upstream adjacent rejoins of the DAA in the west (Figs 4a, c, and f).

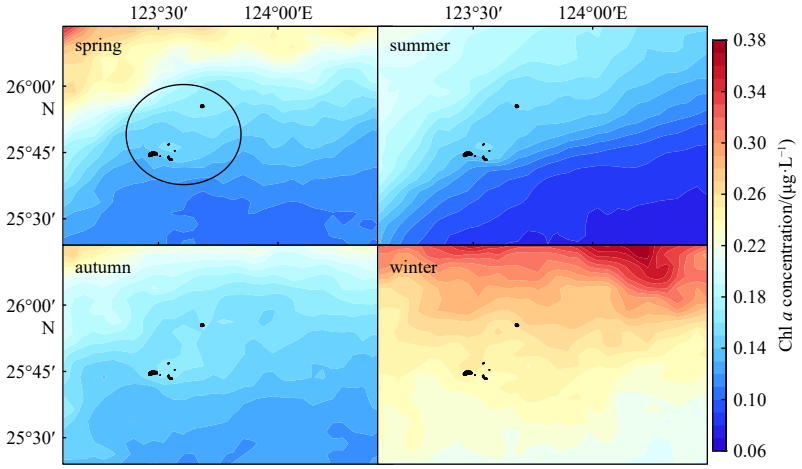

Fig. 2. The distribution of climatology seasonal Chl *a* concentration from MODIS data in the sea around DAA. The location of the DAA is marked by a black circle.

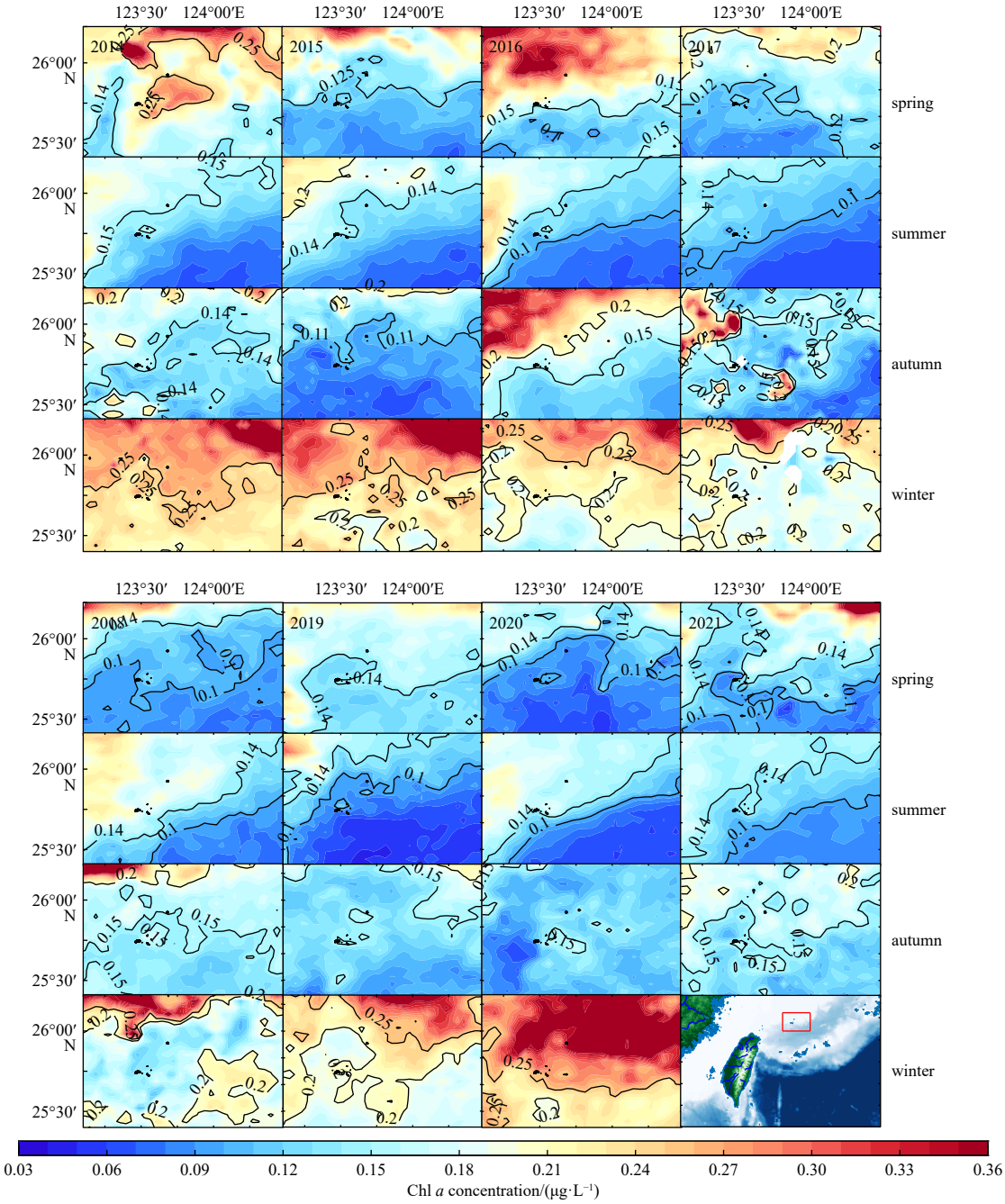

Fig. 3. The seasonal distribution and concentration of Chl *a* in the DAA sea from 2014 to 2021. The column from top to bottom represents spring, summer, autumn, and winter. The real line in the figure represents the isoline of the corresponding value. The location of the general study area is shown in the last subplot by red rectangle. The location of the DAA is marked by a black circle.

4 Discussion

4.1 *Seasonal factors affecting the Chl a concentration in the waters near DAA*

Chl *a* concentration serves as a significant indicator of phytoplankton growth (Xu et al., 2020). Seasonal factors, including SST, currents, wind, and tide, contribute to the variation of Chl *a*. Numerous studies have demonstrated that there is a significant correlation between SST and the alternation and distribution of Chl *a* concentration (Sarmiento et al., 2004). SST is also one of the important driving forces of the IME (Lo-Yat et al., 2011; Uz et al., 2017), and it is found that the corresponding mechanism and results of Chl *a* concentration on SST are not the same in different regions, and may even be the opposite (Dunstan et al., 2018).

DAA is located in the low latitude tropical zone (Fig. 1) that has a temperature exceeding 20℃, which is beneficial to the year-round growth of phytoplankton (Figs 5a–d). The temperature exceeds 28℃ in summer (Fig. 5b), and it falls between 26℃ and 28℃ in spring and

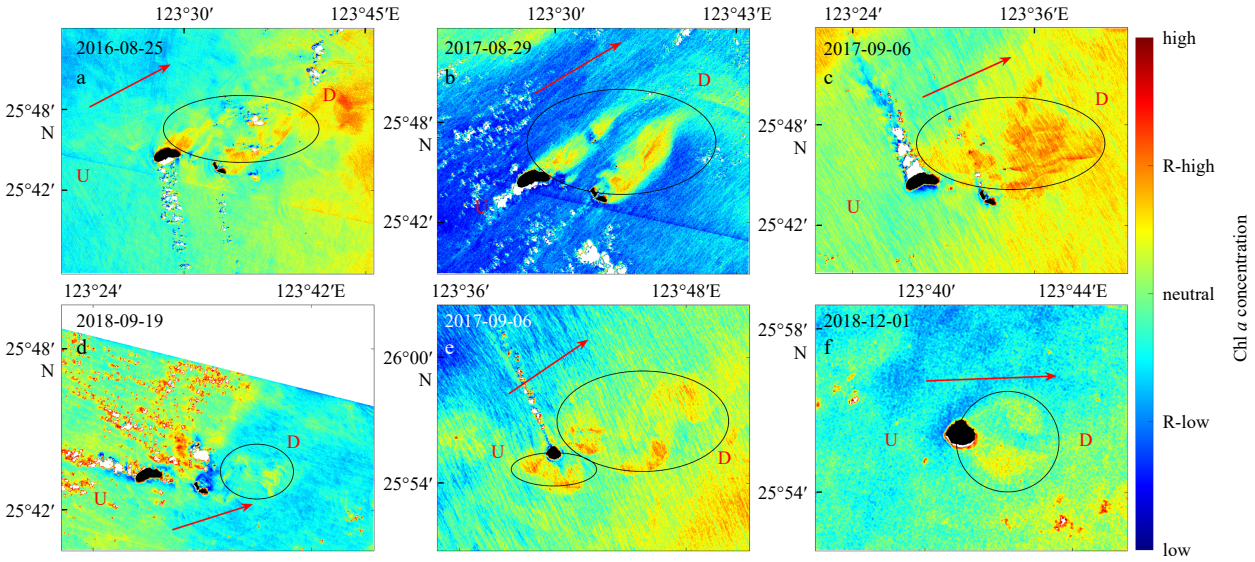

Fig. 4. High-resolution Chl *a* concentration around the DAA obtained from the GF-1 WFV data. The black patch represents the DAA. The color and labels on the color bar represent the qualitative description of Chl *a* concentration in a specific time and space range of the image display, indicating only the relative change degree of Chl *a* concentration. R-low represents relatively low and R-high relatively high. The solid elliptical area marks the IME area. U represents upstream, D downstream, and arrow the direction of the current.

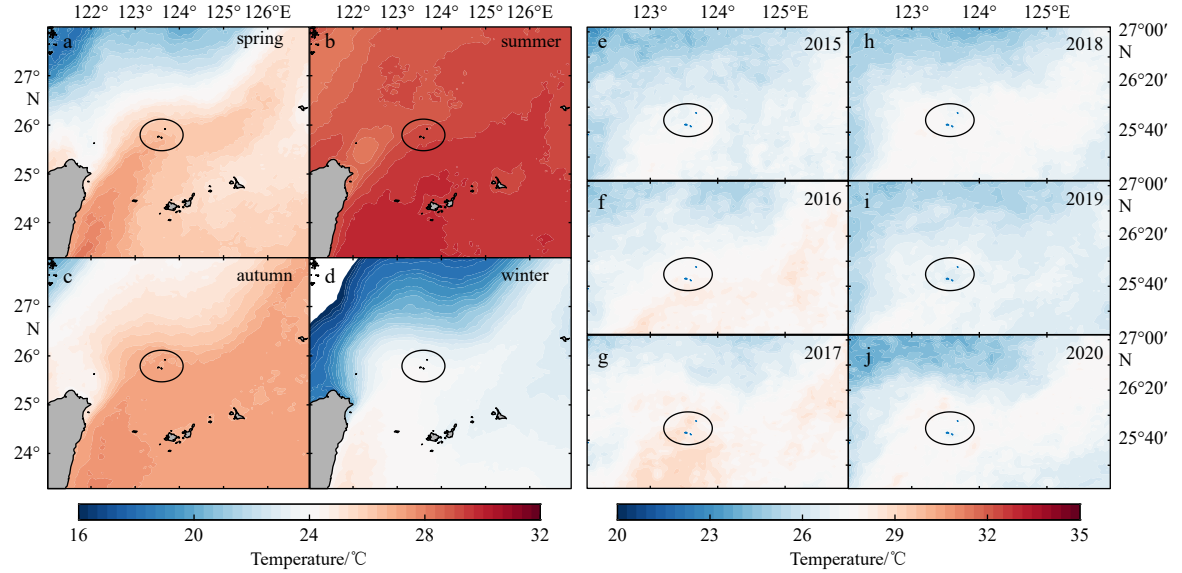

Fig. 5. The seasonal average distribution map of SST from 2002 to 2022 at 24°−28°N (a−d, the black ellipse area is the sea around DAA) and the annual average temperature distribution of the DAA from 2015 to 2020 (e−j, the black ellipse area is the sea around DAA).

autumn (Figs 5a and c), and between 23℃ and 24.5℃ in winter (Fig. 5d). The SST can impact Chl *a* concentration by influencing the stability and stratification of the water column. During the summer and autumn, the increase of SST (Figs 5b and c) will enhance the stability of the water column, prevent the surface water layer from sinking, and weaken the vertical convection, which can cut off the supplement of bottom nutrients to the surface seawater. When the SST decreases in winter (Fig. 5d) and spring (Fig. 5a), the surface cold water sinks, and the lower water with high nutrients rises, causing the deepened MLD and the mixed layer nutrients to increase, thereby stimulating the growth and reproduction of phytoplankton. (Wang et al., 2017; Sarmiento et al., 2004). As increment observed in Fig. 4, the Chl *a* concentration of DAA sea in winter is mostly significantly higher than the other seasons with 0.02−0.05 μg/L (Fig. 3, winter).

The Kuroshio is a robust western boundary current that flows through the waters of the DAA and holds immense ecological significance to the East China Sea (Fig. 6) (Liu et al., 2021; Zuo et al., 2019; Kanayama et al., 2020). The Kuroshio, with a width of 100−150 km, is distin-

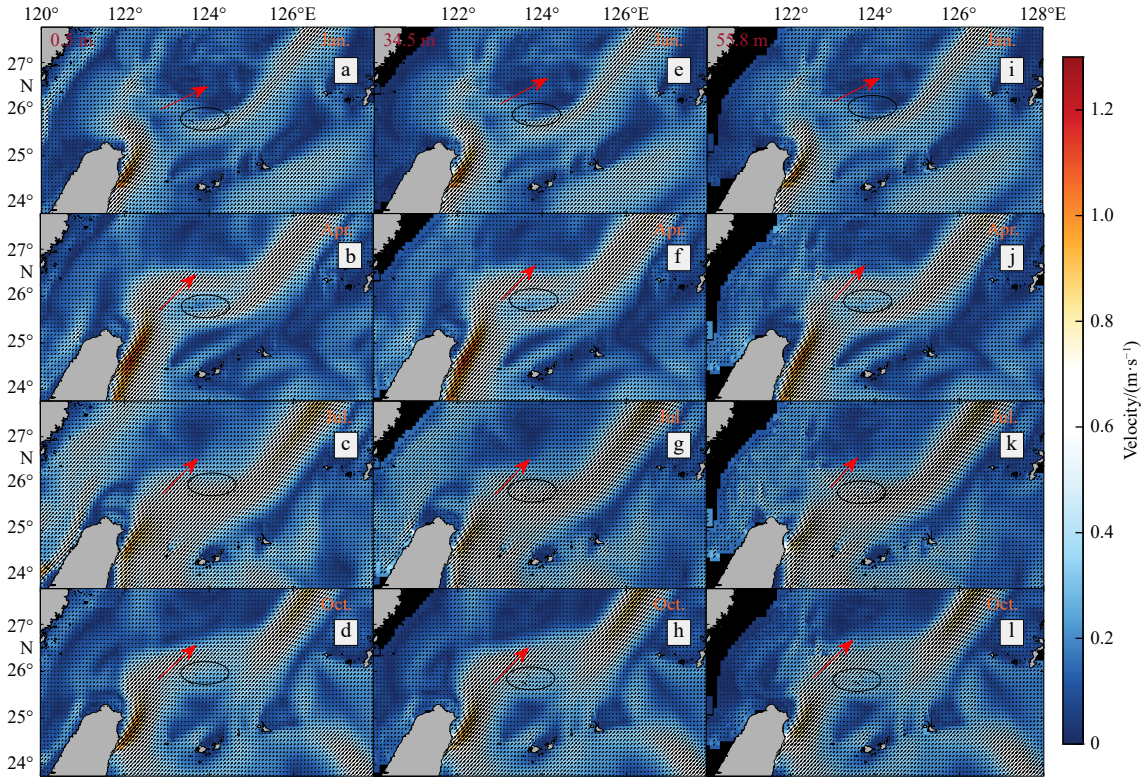

Fig. 6. The current of DAA. The left panel shows the flow field at a depth of 0.5 m below the sea surface. The middle panel shows the flow field at a depth of 34.5 m below the sea surface. The right panel shows the flow field at a depth of 55.8 m below the sea surface. Every column from top to bottom is the average data for January, April, July, and October, representing winter, spring, summer, and autumn respectively. The DAA is located at the solid ellipse mark in the figure. Red arrow means the direction of current.

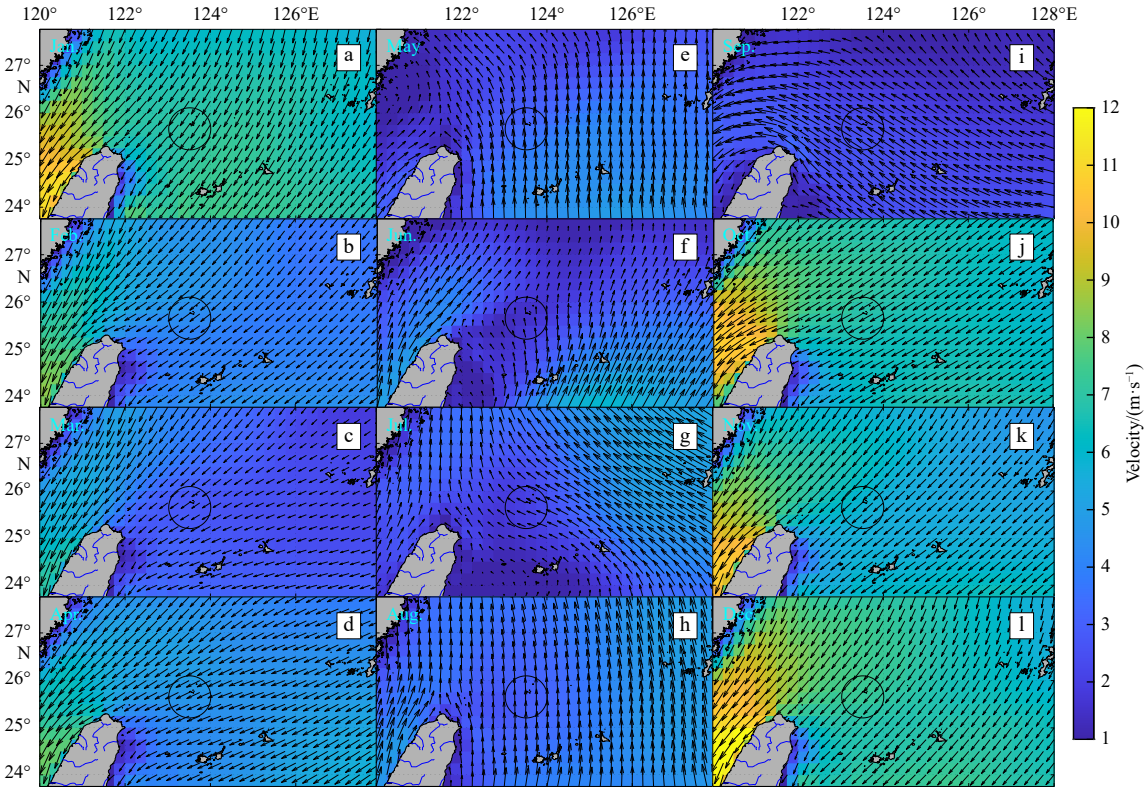

Fig. 7. The DAA's monthly average wind field intensity and direction distribution in 2021. The DAA is located at the solid ellipse mark in the figure.

guished by its high heat and high speed with 0.75−1.5 m/s. It transports a significant amount of water, organic matter, and salt (Kawabe, 1995; Qiu, 2001), and instrument in regulating the nutrient fluxes by bringing rich phosphate for the phosphate-limited ECS, which is crucial to phytoplankton (Wong et al., 1998; Huang et al., 2019).

The flow direction of the Kuroshio in the DAA region is from southwest to east (Fig. 6), which is consistent with the high-value area of Chl *a* in spring of the 2014 and summer of 2018 in Fig. 3 from southwest-northeast to east-west in autumn and winter. The Chl *a* concentration in the region to the west of DAA is lower than that in the eastern and northeastern parts all year around (Figs 3 and 4) showing the same direction as that of the Kuroshio (Fig. 6) in the region around the DAA (Ding et al., 2016). The upper Kuroshio Current, which is found on the northeast coast of the Taiwan Island, periodically shifts its route toward the coastline during autumn (Fig. 6d) and winter (Fig. 6a) and towards the open ocean during spring (Fig. 6b) and summer (Fig. 6c) (Ding et al., 2016). Water intrusion of Kuroshio into the continental shelf of the East China Sea and the corresponding seasonal frequency were analyzed (Wu et al., 2014) and it found that the frequency of intrusion events increases during the winter and spring, and the mechanism of intrusion is related to monsoon and surface heat flux (Wu et al., 2014). The intrusion water often corresponds to a slower flow rate, which is also consistent with the phenomenon observed in Figs 6a and d (Hsin et al., 2013). When it moves to the shallow continental shelf and DAA in autumn and winter, it brings a lot of nutrients (Ji et al., 2023), may foster the growth of phytoplankton in the DAA sea area, and amplifies the concentration of Chl *a*.

Monsoon also plays an important role in the distribution of Chl *a*. The DAA's sea area blows the northeast monsoon in winter (Figs 7a, b, and i) and the southwest monsoon in summer (Figs 7e, f, and j) (Zheng et al., 2014), which weakens and promotes the intensity of the Kuroshio in the opposite and same directions, respectively (Chaot, 1990). May and August are in the stable stage of blowing southernly. It may inhibit the drift and shedding of the vortex induced by the DAA in winter and autumn (Yoshida et al., 2010), resulting in the increase of the residence time of the high nutrient water mass in the sea area near DAA and the concentration of phytoplankton and Chl *a* (Hsu et al., 2015). The range of action of IME is may limited to a certain extent, but the intensity in the sea area near the DAA is enhanced to a certain extent.

4.2 *The influence of DAA on Chl a*

A direct correlation between the DAA and increase in Chl *a* level is obvious (Figs 3 and 4). The IME effect occurs within the DAA area (Andrade et al., 2014a; Arístegui et al., 1994). The islands interact with the atmosphere and ocean currents which induce the changes in local currents and further effect Chl *a* concentration. The island-induced vortex can increase downstream current velocity in various depths (Hsu et al., 2017), potentially intensifying the disturbance and mix, leading to the injection of nutrients to the surface during the Kuroshio intrusion event, which often implies slow current velocity. According to a number of previous numerical simulations and research (Zheng and Zheng, 2014; Hasegawa et al., 2004; Teinturier et al., 2010), the interaction between is-

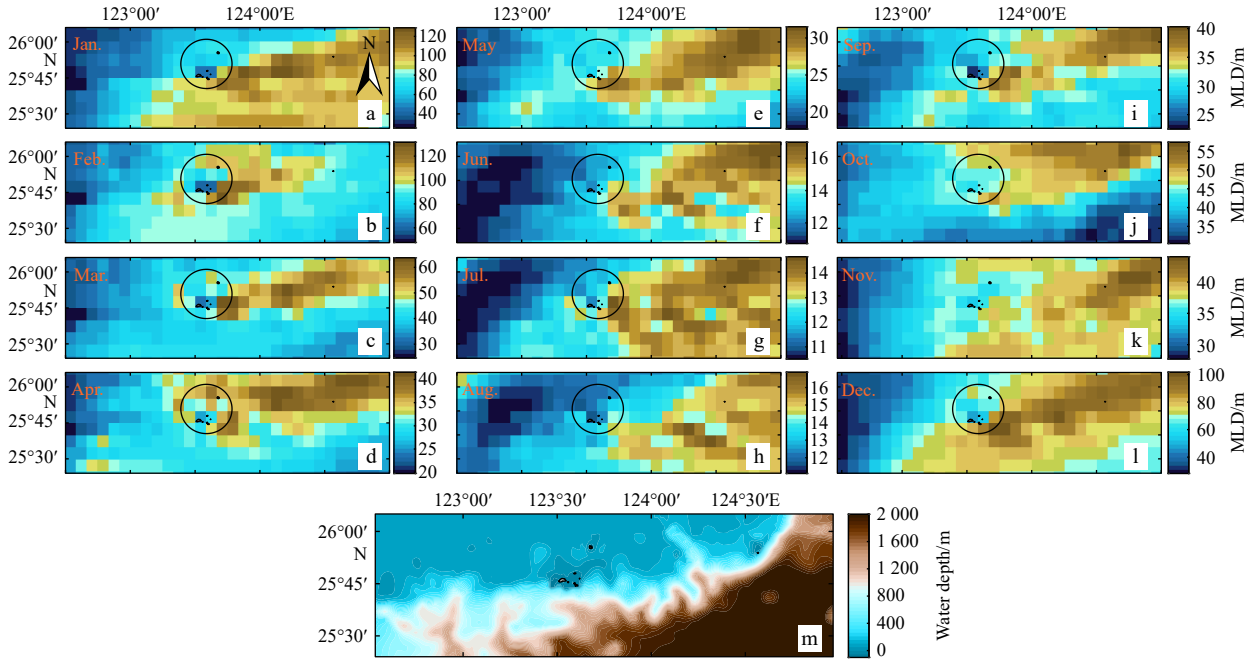

Fig. 8. The MLD contribution map of the sea around the DAA. The upper four rows (a−l) represent the monthly average MLD data, and the lower graph shows the corresponding water depth map for the same geographic extent. The location of the DAA on the map is marked by solid ellipses.

lands and ocean currents or wind fields will induce the Karman vortex street including cyclonic vortices, which can result in sea surface divergence, convection enhancement, and an increase in mixed layer depth, leading to the formation of two dominant patterns that may cause an increase in Chl *a* concentration: (1) Pattern 1. The depth of the maximum Chl *a* (MCD) in the subsurface layer lifted to the surface (Fig. 3, 2018 summer, 2020 summer) by upwelling, which can explain 50% increment of Chl *a* in the presence of this surface maximum value in Kuroshio region by numerical simulation (Gao et al., 2022). (2) Pattern 2. The bottom high nutrient low-temperature water rises to form an upwelling because of the cyclonic vortex, which brings a lot of nutrients to the growth of phytoplankton (Figs 4a–f). Additionally, many background vortices in the Kuroshio region play an important role in regulating the Kuroshio velocity and flow. These mesoscale vortices will interact directly with islands and accelerate the separation and propagation of island-induced vortex (Cardoso et al., 2020).

The DAA plays a significant role in regulating the downstream MLD. As previously mentioned, the MLD reflects the stability of seawater, and the deep seawater plays an important role in the nutrient supply of the surface seawater. The MLD in the northeast coastal waters of DAA is lower throughout the year (Fig. 8), which may be related to the water depth of less than 50 m (Fig. 8m), but it is still significantly deepened in winter (Figs 8a, k, and l), which indicates that the vertical convection process is strengthened in winter. There are obvious seasonal differences in the MLD distribution in the DAA region, the MLD falls between 30 m and 120 m during winter (Figs 8a, b, and l), between 20 m and 60 m during spring and autumn, and between 10 m and 20 m during the summer (Figs 8f, g, and h), which may be attributed to the temperature mentioned earlier. However, the characteristic that the downstream depth is significantly deeper than the upstream is a common phenomenon throughout the year (Fig. 8). According to the comparison of water depth and MLD, the water depth downstream of the DAA is shallower than that of the upstream, but the MLD is evidently on the contrary which is significantly deepened.

The MLD plays an important role in nutrient supply. During winter and spring (December to May), the deeper mixed layer area is more concentrated in the northeastern part of the island (Figs 8e–l). During summer and autumn (June–November) (Figs 8h–k), the deeper mixed layer area is mostly distributed in the eastern part of the island. This shows that the island can make a significant disturbance to the vertical structure of the downstream, resulting in an enhanced vertical movement of the downstream seawater. The upwelling lifts the deep cold water carrying a large amount of nutrients, deepens the mixed layer, weakens the nutrient limitation of surface phytoplankton growth, and induces the increase of Chl *a* concentration in downstream. Based on the diagram, the influence of DAA on the MLD is substantial, significantly exceeding the size of the DAA itself. It is noteworthy that the deepening of the MLD will weaken the maximum Chl *a* concentration in the subsurface, which may weaken the process of Pattern 1 and can explain why the Chl *a* concentration in the DAA sea area generally increases in winter, but the IME effect in the adjacent sea area of the island is not obvious (Fig. 3, winter) (Gao et al., 2022).

4.3 *Other factors*

Other factors such as the background vorticity and the El Niño and La Niña, are also can play an impact on the surrounding environment of the DAA. The background vorticity also plays an important role in the characteristics of the island-induced vortex and the dominant situation of anticyclonic vortex and cyclonic vortex (Stern and Bidlot, 1994; Zhang et al., 1994). The background vorticity around the DAA region is worth being analyzed using more data from field observations and satellites to have a clearer and more comprehensive understanding of the hydrological environment around the DAA.

When El Niño and La Niña events occur, the sea surface temperature will be abnormal. The years of 2015–2016 and 2018–2019 are widely recognized as El Niño years. According to the average temperature map for the period of 2015–2020 (Fig. 5b), it can be observed that the temperature of the DAA area during the El Niño event of 2015–2016 and 2018–2019 (Figs 5e and f) was lower than that of normal years, 2017 and 2020 (Figs 5g and j). This decrease in temperature resulted in a deeper MLD, leading to an increase in Chl *a* concentration. During La Niña events, Chl *a* concentration may decrease due to the thinning of the mixed layer caused by the increase of SST in the DAA sea area (Lo-Yat et al., 2011), which can all have an impact on the IME. Furthermore, the water depth in the DAA is shallow, and the average radius of the vortex in the adjacent area of the island is small. As the vortex propagates to the deepwater area, the residence time of the vortex increases (Cardoso et al., 2020), which may be beneficial to the island to induce delay IME at a long distance (Fig. 3, 2017 autumn) (Signorini et al., 1999; Messié et al., 2020).

The scale of population living is also an important driving force for IME. The nutrients generated and released into the sea by human activities will significantly enhance the development of phytoplankton, which is a very crucial element that impacts the IME in other heavily populated islands (Gove et al., 2016; Vitousek et al., 2008). However, the DAA has a small population, thereby the impact of this factor on the Chl *a* concentration in the DAA sea can be ignored.

4.4 *Suggestions for developing and protecting the DAA*

The interaction between the DAA and the Kuroshio provides conditions for the increase of Chl *a*. Phytoplankton is an important part of the marine nutrition system

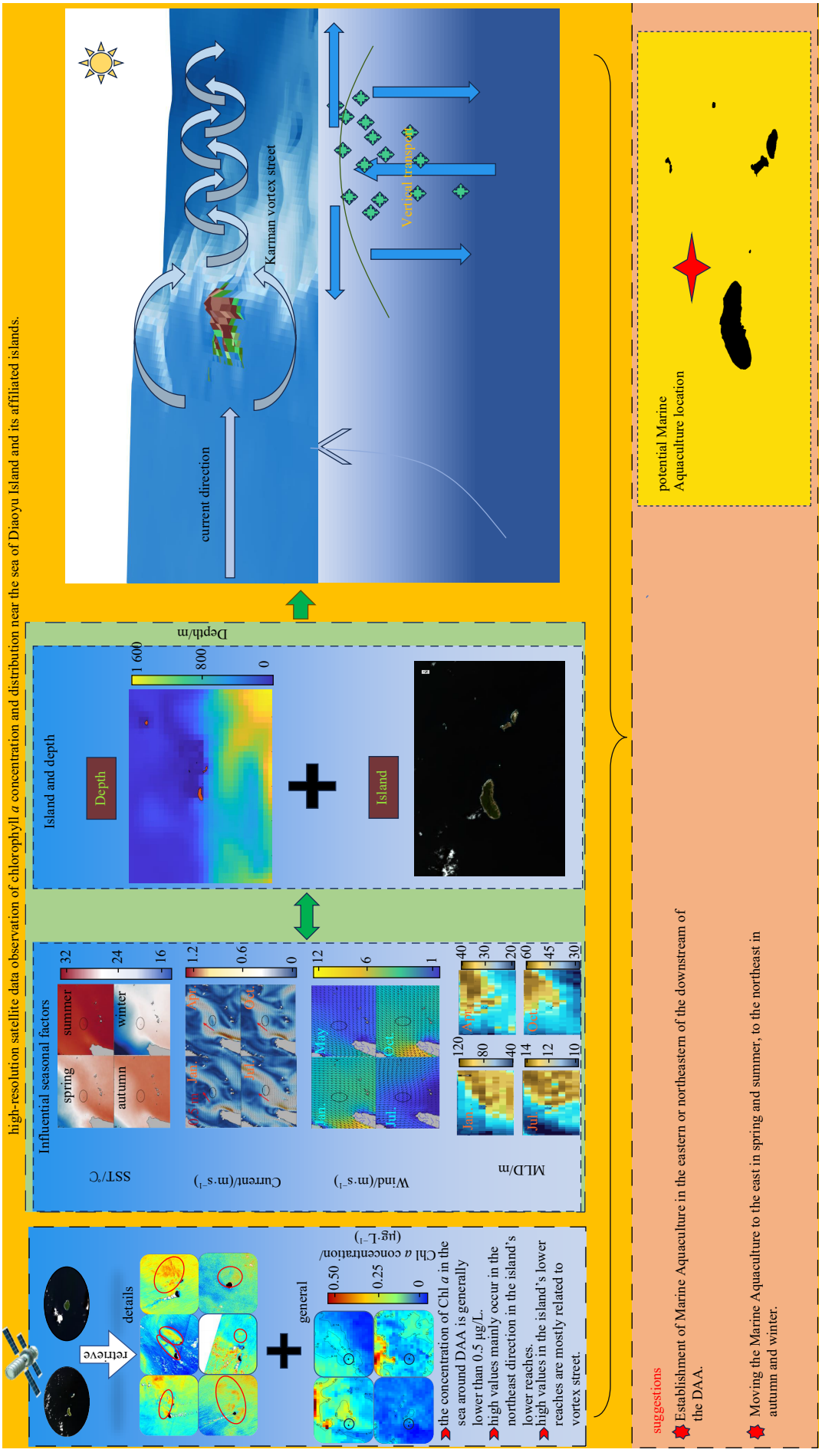

Fig. 9. Graphical abstract of the study.

(Gove et al., 2016). It can determine the distribution and scale of fishery resources and transfer a large number of nutrients to humans through complex and diverse food webs (West et al., 2009). Therefore, the establishment of fishing pastures in the eastern parts of the downstream of the DAA is a scientific and reasonable measure. The stable eastward Kuroshio in the research area leads to the stable presence of high Chl *a* concentration in the downstream vortex street on the east side of DAA. The vertical exchange of active nutrients in the downstream water body on the east side of DAA is abundant, and suitable for the development of fishing pastures such as cage farming. And based on the discovery (Figs 4a–e), the fishing pastures can migrate to the northeast properly in the summer and autumn to use high Chl *a* as much as possible. The upstream of DAA is suitable for developing offshore sports fields or utilizing ocean energy for power generation.

5 Conclusions

High-resolution satellite data reveals the distribution details of Chl *a* concentration in the adjacent waters of DAA. The Chl *a* concentration is between 0.05 and 0.35 μg/L throughout the year, the high values generally distributed in the north and east and the low in the south and west, and the highest value appears in winter. The distribution details of Chl *a* were observed in the upstream and downstream of the DAA. The results suggest the concentration of Chl *a* in the northeast and east directions of the island (downstream) was significantly higher than that in the upstream (west), and there were observed vortexes with high Chl *a* concentration in the downstream of DAA (Fig. 9).

This phenomenon continues to persist in the waters surrounding the DAA. The vortex induced by the interaction between the current and island results in upwelling lifts the maximum Chl *a* concentration layer of the subsurface layer to the surface and replenished a large number of nutrients to the surface, thereby promoting the growth of plankton in the downstream of DAA on the east.

In addition, the DAA plays a significant role in regulating the downstream MLD. In winter and spring, the MLD in the northeast of the downstream is considerably deeper than that in the upstream, and in spring and autumn, the deeper MLD is concentrated in the east of the downstream. The range of influence for the MLD is greatly larger than the size of the island itself, showing that the disruption of the DAA on the current is substantial. In addition, the combined effects of SST and wind also play a significant role in modifying Chl *a*.

Based on the findings of the study, the paper proposes the conception of building fishing pastures downstream of the DAA, and proposes a general migration plan for different seasons to scientifically and rationally utilize the increased Chl *a* concentration downstream of the DAA.

References

Anderson G P, Pukall B, Allred C L, et al. 1999. FLAASH and MODTRAN4: state-of-the-art atmospheric correction for hyperspectral data. In: Proceedings of 1999 IEEE Aerospace Conference. Snowmass: IEEE, 177–181, doi: 10.1109/AERO.1999.792088

Andrade I, Hormazábal S, Correa-Ramírez M. 2014a. Time space variability of satellite chlorophylla in the Easter Island Province, southeastern Pacific Ocean. Latin American Journal of Aquatic Research, 42(4): 871–887, doi: 10.3856/vol42-issue4-fulltext-13

Andrade I, Sangrà P, Hormazabal S, et al. 2014b. Island mass effect in the Juan Fernández Archipelago (33°S), Southeastern Pacific. Deep-Sea Research Part Ⅰ: Oceanographic Research Papers, 84: 86–99, doi: 10.1016/j.dsr.2013.10.009

Arístegui J, Sangrá P, Hernández-León S, et al. 1994. Island-induced eddies in the Canary islands. Deep-Sea Research Part Ⅰ: Oceanographic Research Papers, 41(10): 1509–1525, doi: 10.1016/0967-0637(94)90058-2

Cai Lina, Chen Songyu, Yan Xiaojun, et al. 2022. Study on high-resolution suspended sediment distribution under the influence of coastal zone engineering in the Yangtze River mouth, China. Remote Sensing, 14(3): 486, doi: 10.3390/rs14030486

Cai Lina, Jiang Xiaoqi, Yan Xiaojun, et al. 2023. Study of coexisting upstream solitary wave packet and downstream wakes induced by Diaoyu Dao and its affiliated islands detected by satellite sun glitter. Acta Oceanologica Sinica, 42(4): 1–15, doi: 10.1007/s13131-022-2099-9

Cai Lina, Zhou Minrui, Liu Jianqiang, et al. 2020. HY-1C observations of the impacts of islands on suspended sediment distribution in Zhoushan Coastal Waters, China. Remote Sensing, 12(11): 1766, doi: 10.3390/rs12111766

Cardoso C, Caldeira R M A, Relvas P, et al. 2020. Islands as eddy transformation and generation hotspots: Cabo Verde case study. Progress in Oceanography, 184: 102271, doi: 10.1016/j.pocean.2020.102271

Chaot S Y. 1990. Circulation of the East China Sea, a numerical study. Journal of the Oceanographical Society of Japan, 46(6): 273–295, doi: 10.1007/BF02123503

Chiswell S M, O'Callaghan J M. 2021. Long-term trends in the frequency and magnitude of upwelling along the West Coast of the South Island, New Zealand, and the impact on primary production. New Zealand Journal of Marine and Freshwater Research, 55(1): 177–198, doi: 10.1080/00288330.2020.1865416

Ding Ruibin, Huang Daji, Xuan Jiliang, et al. 2016. Cross-shelf water exchange in the East China Sea as estimated by satellite altimetry and *in situ* hydrographic measurement. Journal of Geophysical Research: Oceans, 121(9): 7192–7211, doi: 10.1002/2016JC011972

Doty M, Oguri M. 1956. The island mass effect. ICES Journal of Marine Science, 22(1): 33–37, doi: 10.1093/icesjms/22.1.33

Dunstan P K, Foster S D, King E, et al. 2018. Global patterns of change and variation in sea surface temperature and chlorophyll *a*. Scientific Reports, 8(1): 14624, doi: 10.1038/s41598-018-33057-y

Felde G W, Anderson G P, Cooley T W, et al. 2003. Analysis of hyperion data with the FLAASH atmospheric correction algorithm. In: Proceedings of IGARSS 2003. 2003 IEEE International Geoscience and Remote Sensing Symposium. Toulouse: IEEE, 90–92

Gao Jie, Guo Xinyu, Yoshie N, et al. 2022. Occurrence of surface phytoplankton bloom as the Kuroshio current passes an island. Journal of Geophysical Research: Oceans, 127(9): e2021JC018242, doi: 10.1029/2021JC018242

Gove J M, McManus M A, Neuheimer A B, et al. 2016. Near-island biological hotspots in barren ocean basins. Nature Communications, 7(1): 10581, doi: 10.1038/ncomms10581

Hasegawa D, Lewis M R, Gangopadhyay A. 2009. How islands cause phytoplankton to bloom in their wakes. Geophysical Research Letters, 36(20): L20605, doi: 10.1029/2009gl039743

Hasegawa D, Yamazaki H, Ishimaru T, et al. 2008. Apparent phytoplankton bloom due to island mass effect. Journal of Marine Systems, 69(3–4): 238–246, doi: 10.1016/j.jmarsys.2006.04.019

Hasegawa D, Yamazaki H, Lueck R G, et al. 2004. How islands stir and fertilize the upper ocean. Geophysical Research Letters, 31(16): L16303, doi: 10.1029/2004gl020143

Hsin Yi-Chia, Qiu Bo, Chiang Tzu-Ling, et al. 2013. Seasonal to interannual variations in the intensity and central position of the surface Kuroshio east of Taiwan. Journal of Geophysical Research: Oceans, 118(9): 4305–4316, doi: 10.1002/jgrc.20323

Hsu Po-Chun, Chang Ming-Huei, Lin Chen-Chih, et al. 2017. Investigation of the island-induced ocean vortex train of the Kuroshio Current using satellite imagery. Remote Sensing of Environment, 193: 54–64, doi: 10.1016/j.rse.2017.02.025

Hsu Tai-Wen, Doong Dong-Jiing, Hsieh Kai-Jiun, et al. 2015. Numerical study of monsoon effect on green island wake. Journal of Coastal Research, 315: 1141–1150, doi: 10.2112/jcoastres-d-14-00206.1

Huang Ting-Hsuan, Chen Chen-Tung Arthur, Lee Jay, et al. 2019. East China Sea increasingly gains limiting nutrient P from South China Sea. Scientific Reports, 9(1): 5648, doi: 10.1038/s41598-019-42020-4

Ji Chongxiao, Yang Guipeng, Chen Yan, et al. 2023. Contrast the distribution, transformation, and degradation of dissolved and particulate organic matter in the South Yellow Sea, the East China Sea, and its adjacent Kuroshio Current. Marine Chemistry, 248: 104210, doi: 10.1016/j.marchem.2023.104210

Kanayama T, Kobari T, Suzuki K, et al. 2020. Impact of microzooplankton grazing on the phytoplankton community in the Kuroshio of the East China sea: a major trophic pathway of the Kuroshio ecosystem. Deep-Sea Research Part Ⅰ: Oceanographic Research Papers, 163: 103337, doi: 10.1016/j.dsr.2020.103337

Kawabe M. 1995. Variations of current path, velocity, and volume transport of the Kuroshio in relation with the large meander. Journal of Physical Oceanography, 25(12): 3103–3117, doi: 10.1175/1520-0485(1995)025<3103:VOCPVA>2.0.CO;2

Lamont T, Toolsee T. 2022. Spatial and seasonal variations of the island mass effect at the sub-antarctic prince edward islands archipelago. Remote Sensing, 14(9): 2140, doi: 10.3390/rs14092140

Liu Chih-Lun, Chang Ming-Huei. 2018. Numerical studies of submesoscale island wakes in the Kuroshio. Journal of Geophysical Research: Oceans, 123(8): 5669–5687, doi: 10.1029/2017JC013501

Liu Z Q, Gan J P, Hu J Y, et al. 2021. Progress on circulation dynamics in the East China Sea and southern Yellow Sea: origination, pathways, and destinations of shelf currents. Progress in Oceanography, 193: 102553, doi: 10.1016/j.pocean.2021.102553

Lo-Yat A, Simpson S D, Meekan M, et al. 2011. Extreme climatic events reduce ocean productivity and larval supply in a tropical reef ecosystem. Global Change Biology, 17(4): 1695–1702, doi: 10.1111/j.1365-2486.2010.02355.x

Ma Caihua, You Kui, Liu Yuxin. 2012. Study on the marine resources value over Diaoyu Islands. Chinese Fisheries Economics (in Chinese), 30(6): 125–129

Mattei F, Scardi M. 2022. Mining satellite data for extracting chlorophyll a spatio-temporal patterns in the Mediterranean Sea. Environmental Modelling & Software, 150: 105353, doi: 10.1016/j.envsoft.2022.105353

Messié M, Petrenko A, Doglioli A M, et al. 2020. The delayed island mass effect: how islands can remotely trigger blooms in the oligotrophic ocean. Geophysical Research Letters, 47(2): e2019GL085282, doi: 10.1029/2019GL085282

Nielsen R, Hoff A, Waldo S, et al. 2019. Fishing for nutrients—economic effects of fisheries management targeting eutrophication in the Baltic Sea. Ecological Economics, 160: 156–167, doi: 10.1016/j.ecolecon.2019.02.013

Peng Jida, Zhang Chungui. 2019. Remote sensing monitoring of vegetation coverage by GF-1 satellite: a case study in Xiamen City. Remote Sensing for Land & Resources, 31(4): 137–142, doi: 10.6046/gtzyyg.2019.04.18

Qin Xianlin, Yang Fei, Zu Xiaofeng, et al. 2014. Quantitative extraction of fine contour parameters for forest fire using satellite remote sensing. Journal of Infrared and Millimeter Waves, 33(6): 642–648, doi: 10.11972/j.issn.1001-9014.2014.06.013

Qiu Bo. 2001. Kuroshio and Oyashio currents. In: Steele J H, ed. Encyclopedia of Ocean Sciences. Oxford: Academic Press, 1413–1425

Rosa A, Cardoso C, Vieira R, et al. 2022. Impact of flash flood events on the coastal waters around madeira island: the

"Land Mass Effect". Frontiers in Marine Science, 8: 749638, doi: 10.3389/fmars.2021.749638

Roxy M K, Modi A, Murtugudde R, et al. 2016. A reduction in marine primary productivity driven by rapid warming over the tropical Indian Ocean. Geophysical Research Letters, 43(2): 826–833, doi: 10.1002/2015gl066979

Sarmiento J L, Slater R, Barber R, et al. 2004. Response of ocean ecosystems to climate warming. Global Biogeochemical Cycles, 18(3): GB3003, doi: 10.1029/2003gb002134

Shang S L, Dong Q, Hu C M, et al. 2014. On the consistency of MODIS chlorophyll *a* products in the northern South China Sea. Biogeosciences, 11(2): 269–280, doi: 10.5194/bg-11-269-2014

Signorini S R, McClain C R, Dandonneau Y. 1999. Mixing and phytoplankton bloom in the wake of the Marquesas Islands. Geophysical Research Letters, 26(20): 3121–3124, doi: 10.1029/1999GL010470

Song Kaishan, Li Lin, Wang Zongming, et al. 2012. Retrieval of total suspended matter (TSM) and chlorophyll-*a* (Chl-*a*) concentration from remote-sensing data for drinking water resources. Environmental Monitoring and Assessment, 184(3): 1449–1470, doi: 10.1007/s10661-011-2053-3

Stern M E, Bidlot J R. 1994. Lateral entrainment in baroclinic currents. Journal of Marine Research, 52(1): 25–53, doi: 10.1357/0022240943076786

Teinturier S, Stegner A, Didelle H, et al. 2010. Small-scale instabilities of an island wake flow in a rotating shallow-water layer. Dynamics of Atmospheres and Oceans, 49(1): 1–24, doi: 10.1016/j.dynatmoce.2008.10.006

Uz S S, Busalacchi A J, Smith T M, et al. 2017. Interannual and decadal variability in tropical Pacific chlorophyll from a statistical reconstruction: 1958–2008. Journal of Climate, 30(18): 7293–7315, doi: 10.1175/JCLI-D-16-0202.1

Vitousek P M, Mooney H A, Lubchenco J, et al. 2008. Human domination of earth's ecosystems. In: Marzluff J M, Shulenberger E, Endlicher W, et al., eds. Urban Ecology: An International Perspective on the Interaction Between Humans and Nature. Boston, MA: Springer, 3–13

Vollbrecht C, Moehlenkamp P, Gove J M, et al. 2021. Long-term presence of the island mass effect at rangiroa atoll, french polynesia. Frontiers in Marine Science, 7: 595294, doi: 10.3389/fmars.2020.595294

Wang Teng, Liu Guangpeng, Gao Lei, et al. 2017. Biological responses to nine powerful typhoons in the East China Sea. Regional Environmental Change, 17(2): 465–476, doi: 10.1007/s10113-016-1025-0

West E J, Pitt K A, Welsh D T, et al. 2009. Top-down and bottom-up influences of jellyfish on primary productivity and planktonic assemblages. Limnology and Oceanography, 54(6): 2058–2071, doi: 10.4319/lo.2009.54.6.2058

Wong G T F, Gong G C, Liu K K, et al. 1998. 'Excess Nitrate' in the East China Sea. Estuarine, Coastal and Shelf Science, 46(3): 411–418

Wu Chau-Ron, Hsin Yi-Chia, Chiang Tzu-Ling, et al. 2014. Seasonal and interannual changes of the Kuroshio intrusion onto the East China Sea Shelf. Journal of Geophysical Research: Oceans, 119(8): 5039–5051, doi: 10.1002/2013jc009748

Xu Jian, Gao Chen, Wang Yeqiao. 2020. Extraction of spatial and temporal patterns of concentrations of chlorophyll-*a* and total suspended matter in poyang lake using GF-1 satellite data. Remote Sensing, 12(4): 622, doi: 10.3390/rs12040622

Xu Yongjiu, Jiang Rijin, Hao Qiang, et al. 2019. Effects of environmental change and exploitation on marine communities around the Zhoushan archipelago: a functional group perspective. Estuarine, Coastal and Shelf Science, 217: 185–195, doi: 10.1016/j.ecss.2018.11.015

Yoshida S, Qiu Bo, Hacker P. 2010. Wind-generated eddy characteristics in the lee of the island of Hawaii. Journal of Geophysical Research: Oceans, 115(C3): C03019, doi: 10.1029/2009jc005417

Zhang Xiuzhang, McGuinness D S, Boyer D L. 1994. Narrow barotropic currents impinging on an isolated seamount. Journal of Geophysical Research: Oceans, 99(C11): 22707–22724, doi: 10.1029/94JC01569

Zheng Guizhou, Li Chunyan. 2022. An empirical algorithm for retrieving chlorophyll-*a* concentration in the sea area near Palawan Island. Science of Surveying and Mapping (in Chinese), 47(5): 168–176

Zheng Chongwei, You Xiaobao, Pan Jing, et al. 2014. Feasibility analysis on the wind energy and wave energy resources exploitation in Fishing Islands and Scarborough Shoal. Marine Forecasts (in Chinese), 31(1): 49–57, doi: 10.11737/j.issn.1003-0239.2014.01.008

Zheng Zhewen, Zheng Quanan. 2014. Variability of island-induced ocean vortex trains, in the Kuroshio region southeast of Taiwan Island. Continental Shelf Research, 81: 1–6, doi: 10.1016/j.csr.2014.02.010

Zuo Jiulong, Song Jinming, Yuan Huamao, et al. 2019. Impact of Kuroshio on the dissolved oxygen in the East China Sea region. Journal of Oceanology and Limnology, 37(2): 513–524, doi: 10.1007/s00343-019-7389-5